LAWRENCE
LIVERMORE
NATIONAL
LABORATORY

LLNL-PROC-424642

Observation of off-Hugoniot shocked states with ultrafast time resolution

M. Armstrong, J. Crowhurst, S. Bastea, J. Zaug

February 26, 2010

International Detonation Symposium
Coeur d'Alene, ID, United States
April 11, 2010 through April 16, 2010

Disclaimer

Observation of off-Hugoniot shocked states with ultrafast time resolution

Michael R. Armstrong, Jonathan C. Crowhurst, Sorin Bastea, and Joseph M. Zaug

Physical and Life Sciences Directorate
Lawrence Livermore National Laboratory, Livermore, California 94550, USA

Abstract. We apply ultrafast single shot interferometry to determine the pressure and density of argon shocked from up to 7.8 GPa static initial pressure in a diamond anvil cell. This method enables the observation of thermodynamic states distinct from those observed in either single shock or isothermal compression experiments, and the observation of ultrafast dynamics in shocked materials. We also present a straightforward method for interpreting ultrafast shock wave data which determines the index of refraction at the shock front, and the particle and shock velocities for shock waves in transparent materials. Based on these methods, we observe shocked thermodynamic states between the room temperature isotherm of argon and the shock adiabat of cryogenic argon at final shock pressures up to 28 GPa.

Introduction

For decades, compression experiments have been used to determine thermodynamic states of materials at high pressure and temperature. Such data are necessary to correctly interpret seismic data[1,2], understand planetary composition[3], the evolution of the early solar system[4], shock wave induced chemistry[5], and fundamental issues in condensed matter physics[6-8]. Most compression experiments have applied either static compression in a diamond anvil cell (DAC)[9-13], or dynamic compression using shock waves[6]. Broadly, these methods obtain material properties along two one-dimensional trajectories in thermodynamic phase space – the isotherm (via static compression) and the shock adiabat, or Hugoniot. Although highly dependent on the sample and the specific method, generally DAC methods obtain relatively low temperature, isothermal compression at less than ~400 GPa pressure. In contrast, single shock methods have obtained much higher pressure (well into the TPa range), typically at much higher temperature. Although such experiments provide a wide range of material data, special techniques are required to obtain information about intermediate pressures and temperatures[6,9,14,15]. In particular, for single shock compression of highly compressible materials from ambient pressure, the density approaches a constant with increasing shock pressure[6,15], limiting the application of single shock methods to low density states. Here we demonstrate the generation and characterization of shock waves on an ultrafast time scale in samples compressed in a conventional diamond anvil cell, under an initial static pressure up to 7.8 GPa. This method enables the investigation of compressed states off the room temperature Hugoniot and the room temperature isotherm, which are challenging to obtain using static or single shock wave compression.

Shock compression of a precompressed material enables two powerful experimental strategies. Single shock experiments provide equation of state information along a one-

dimensional trajectory in pressure-density space: the shock adiabat, or Hugoniot. Since the Hugoniot depends on the initial thermodynamic state of the material, by varying the initial density through applied precompression it is possible to obtain different Hugoniots as a function of initial conditions. Generally, upon shock compression, a material initially at low density will heat more substantially than it would if it were initially at higher density. Thus, by isothermally precompressing the material the final temperature of the shocked state can be decreased and the final density increased, enabling the characterization of thermodynamic states off the principal Hugoniot (i.e. the Hugoniot whose initial density is the most common for the material in question[6]). This method has previously been applied in large-scale laser shock experiments on longer time scales at precompression in the range of ~1 GPa[15].

Isothermal compression in a diamond anvil cell is a very effective way to control the initial density. For instance, solid argon changes in density by only 8% between 0 K and its boiling point at 1 bar. In contrast, argon under isothermal compression exhibits a ~4x density increase from 0.1 to 33 GPa[16] applied pressure.

Also, the initial state of the material can be placed, via precompression (preheating may also be used), in the proximity of a phase transition or chemical reaction boundary before shock compression, enabling the observation of phase transition or chemical dynamics as the material is shock compressed across the boundary. We note that, in cases where shock induced chemistry or phase transitions do not occur, shock compression obtains equilibrium compressed states over picosecond time scales[6]. When materials undergo structural changes upon compression, shock compression can be used to obtain ultrafast dynamic information from shocked metastable compressed states en route through a phase transition or chemistry. Such experiments can provide valuable information on early time states of shocked materials, such as the pre-chemistry shocked Hugoniot of reactive materials, or anomalous transient states preceding phase transitions[17]. Although ultrafast methods have been applied to investigate shock induced chemistry[18,19] from ambient pressure, acoustics in the DAC[20], and shock waves starting from ambient pressure[21,22], shock waves have not been observed in precompressed materials with ultrafast time resolution.

Experimental method

An experimental schematic diagram is shown in fig. 1. In this study, the initial density of preshocked argon ranges from 1.65 g/cc (for cryogenic liquid argon) to 2.8 g/cc (at 7.8 GPa and room temperature). To initiate shock compression of the sample, a ~300 ps, 800 nm center wavelength, ~25 nm bandwidth, ~100-300 μJ pump pulse with a less than 10 ps duration initial rise time is focused to a spot size ranging (depending on the experiment) from 20 μm to 50 μm FWHM intensity diameter at the diamond interface of a ~1 μm thick aluminum layer which partially coats one culet of one diamond in the DAC. Plasma expansion of the ablated aluminum layer drives a shock wave into the precompressed sample[23].

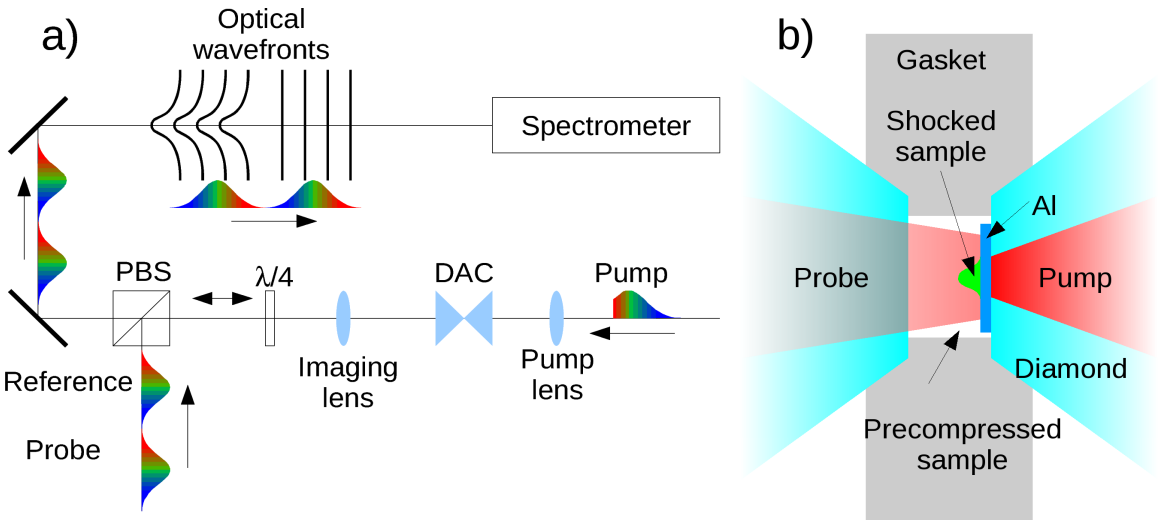

Fig. 1. The experimental setup, a) shows the optical setup external to the DAC and b) shows a close up of a cross section of the DAC, where precompressed sample is shocked via ablation of a ~1 micron aluminum layer on the culet of the right side diamond.

The shock and particle velocities are measured via interferometry using broadband, linearly chirped probe and reference pulses (with the same spectral characteristics as the pump) separated in time by 10 ps – a method that is the ultrafast analog to the velocity interferometry system for any reflector (VISAR) used to characterize shock waves on longer time scales[24]. The probe and reference pulses are chirped to provide a ~250 ps window with 2-3 ps intrinsic time resolution[25]. In this work, an additional moving window average is applied to the data, reducing the time resolution to 10 ps. Time resolution is obtained by spectrally resolving interference between the probe and reference in a way that is analogous to ultrafast time resolution shock characterization methods used previously[21,26,27].

A schematic of the pump-probe geometry and a picture of the sample region in a DAC after an experiment is shown in fig. 2. This experimental setup is similar to that used in previous work[20,28], but in this case using chirped pulses. The surface of the sample is imaged at a numerical aperture of 0.3 with a total magnification of ~10x onto the slit of an imaging spectrometer, with the probe/reference and pump profiles centered on the spectrometer slit. The slit width is typically ~20 μm, corresponding to the CCD pixel width and a 2 μm width at the sample plane. The pump is focused with a relatively high numerical aperture of ~0.1 to avoid self-focusing before it reaches the ablator. The pump waist is typically 200-500 μm downstream from the ablator to achieve a 20-50 μm pump spot size (FWHM intensity) at the ablator. A 10 ps time delay between the probe and reference results in intensity beating in the spectrum, with ~100 fringes over the 22 nm/1340 pixel spectral range of the spectrometer. This intensity beating records a time/wavelength dependent phase shift between the probe and reference which occurs during the 10 ps probe/reference delay. The phase of the intensity profile is recovered using the method of Kim et al.[29] and the phase shift due to shock wave

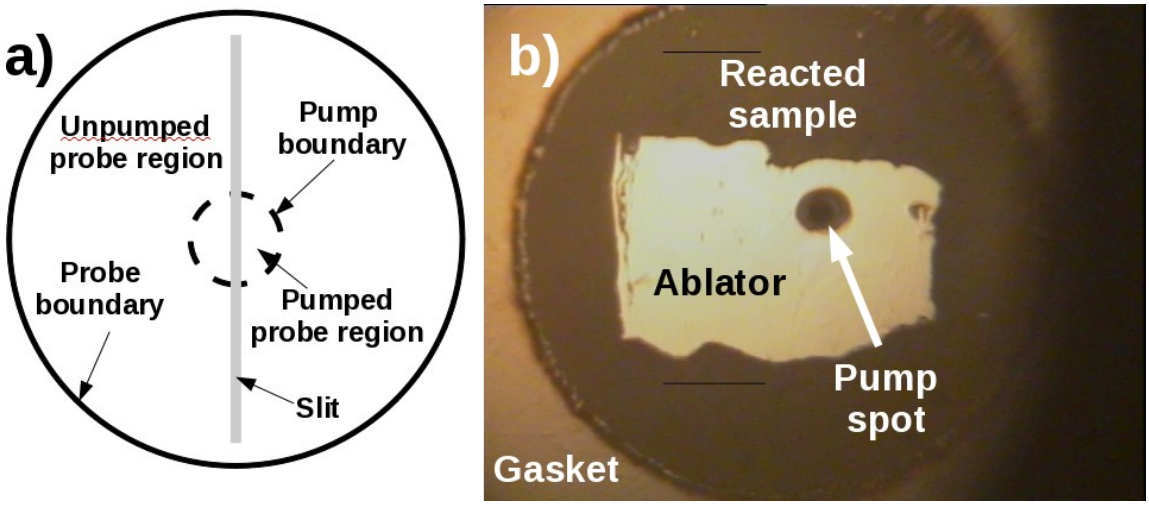

Fig. 2: a) A schematic of the pump and probe/reference imaged at the spectrometer slit and b) an image of DAC from the pump side after an experiment. In this case, the sample was nitromethane, which reacted during the experiment and produced a black product which filled the DAC sample cavity. Although the reaction in this experiment was pump induced, it was not obviously correlated with interferometric probe data within 250 ps after the pump, and may have occurred after the probe time window. The short black horizontal line segments are camera artifacts.

injection into the sample is obtained by taking the phase shift difference between pumped and unpumped regions of the sample, analogous to the method of Gahagan et al.[28] In the case of a metal surface expanding into vacuum (i.e. when the probe does not traverse shocked material), a measured phase offset gives the surface velocity via the same expression as used in VISAR[24], i.e.,

$$surface\ velocity = \frac{\lambda}{4\pi}\frac{\Delta\phi}{\Delta t} \quad , \qquad (1)$$

where λ is the probe wavelength and Δt is the probe/reference delay. Such data are directly analogous to VISAR phase shift measurements taken on longer time scales.

Since the time scale of the experiment is relatively short (100s of ps), the pump is focused to a small spot size without compromising the 1D planar shock wave approximation. In particular, the shock breakout profiles are self-similar subsequent to shock arrival, indicating that shock curvature does not play a strong role in the shock propagation over the time scale of the experiment. We estimate the shock curvature to be sufficiently large (~mm) compared with the propagation distance (which is typically less than one micron) to assume 1D wave propagation.

When a transparent material is shocked, as shown schematically in fig. 3a, the shock front acts as a moving dielectric mirror, partially reflecting and Doppler shifting probe light. The moving metal ablation layer also Doppler shifts reflected probe light, and optical beating between these two reflections results in a high frequency (> 10 GHz) oscillation in the phase, which is not detected in VISAR experiments (which typically have greater than 100 ps time resolution). An example of phase shift data obtained from argon shocked from an initial pressure of 7.8 GPa is shown in fig. 3b. These data are described by an offset added to a sinusoidal oscillation. Because the probe now

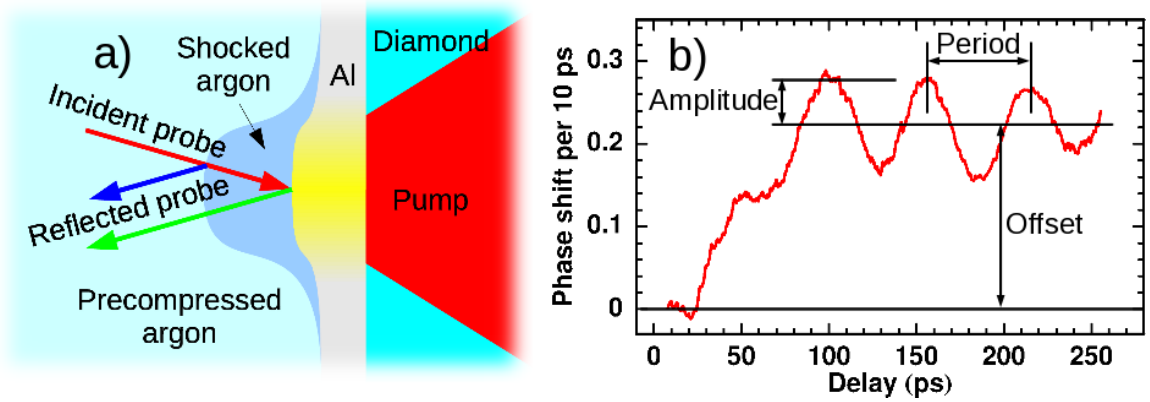

Fig. 3: a) A schematic of the probe/reference interaction with the shocked region. Although only the first probe reflection from the shock front is shown, the shocked region is a dielectric film with multiple internal reflections of the probe. For a sufficiently small index rise at the shock front (< 0.9 for compressed argon with a precompressed index of ~1.4), only the first order reflections need be considered. The pump diameter is much larger than the distance the shock wave travels over the duration of the experiment. b) An example of the shock induced phase shift data in argon precompressed to 7.8 GPa, with a description of the parameterization.

traverses a shocked region with a different index of refraction than the unshocked region, the phase offset now includes a contribution from the advancing shock front in addition to surface motion of the ablator.

To derive shock parameters from these experiments, we expand the optical reflectivity of the shocked region to first order in terms of the reflectivity of the shock front, which is assumed to be a thin optical interface (i.e. the probe wavelength is much larger than the longitudinal extent of the shock front, consistent with previous work[21]).

Given three measured parameters from the phase shift data (as shown in fig. 3b): the offset ($\Delta\theta_m$), period (τ), and oscillation amplitude ($\Delta\delta_{max}$), we calculate the shock velocity (v_s), particle velocity (v_p), and index of refraction behind the shock front (n_s) via the following relations:

$$
\begin{aligned}
\delta_{max} &= \frac{\tau}{2\pi}\frac{\Delta\delta_{max}}{\Delta t} \\
|r_s| &= \delta_{max}\frac{|r_m|}{1+|r_m|^2} \\
\Delta n &= \frac{2n_0|r_s|}{1-|r_s|} \\
n_s &= n_0 + \Delta n \\
v_s &= \frac{\lambda}{4\pi n_0}\left[\frac{\Delta\theta_m}{\Delta t}+\frac{2\pi}{\tau}\right] \\
v_p &= \frac{\lambda}{4\pi n_0}\left[\frac{\Delta\theta_m}{\Delta t}+\frac{2\pi}{\tau}\left(1-\frac{n_0}{n_s}\right)\right]
\end{aligned}
\qquad (2)
$$

The data are analyzed by fitting to a quadratic function, which is then subtracted from the signal, leaving a sinusoid. The sinusoid is fitted to determine τ and $\Delta\delta_{max}$, and an average

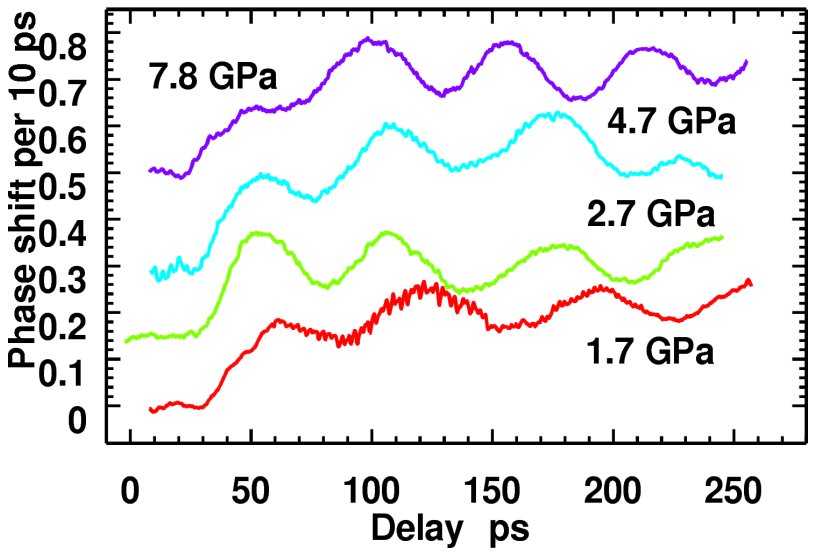

Fig. 4: Shock induced phase shift data taken at precompressions labeled by initial pressure. The data are vertically offset for clarity.

of the quadratic function (which is mostly a constant) to determine the offset, $\Delta\theta_m$. The magnitude of the reflectivity of the ablator (r_m), is generally close to 1.

Results

Raw phase shift data from argon shocked from initial pressures up to 7.8 GPa are shown in fig. 4, with the data traces labeled by initial pressure. We assume the refractive index of shock compressed argon is real. The index of refraction of shock compressed argon in this study should not have a significant imaginary component.

The pressure and density of the shocked state are calculated via the usual methods of shock compression[6], given by:

$$\rho_s = \rho_0 \frac{v_s}{v_s - v_p} \qquad P_s = P_0 + \rho_0 v_s v_p \quad (3)$$

where P_0 , ρ_0 are the initial pressure and density, respectively, and P_s , ρ_s are the shocked pressure and density, respectively.

A plot of the measured thermodynamic states of the shocked argon in pressure-density space is shown in fig. 5. Also shown for comparison are the Hugoniot of liquid cryogenic argon (84 K)[30], the solid argon room temperature isotherm[16], and the calculated boundaries of the solid and liquid equilibrium phases of argon. The calculations were performed using fluid and solid variational theories[31,32] with the exp-6 potential developed by Ross[33], which reproduce very well the experimental Hugoniot, room temperature isotherm and melting line of argon. The parameters of the signal (offset, amplitude, and period) do not strongly vary, supporting the supposition of a steady shock wave over the duration of the experiment. We also obtained shock data from cryogenic liquid argon at 84 K, which is quite consistent with the Hugoniot derived from gas gun based measurements[30],

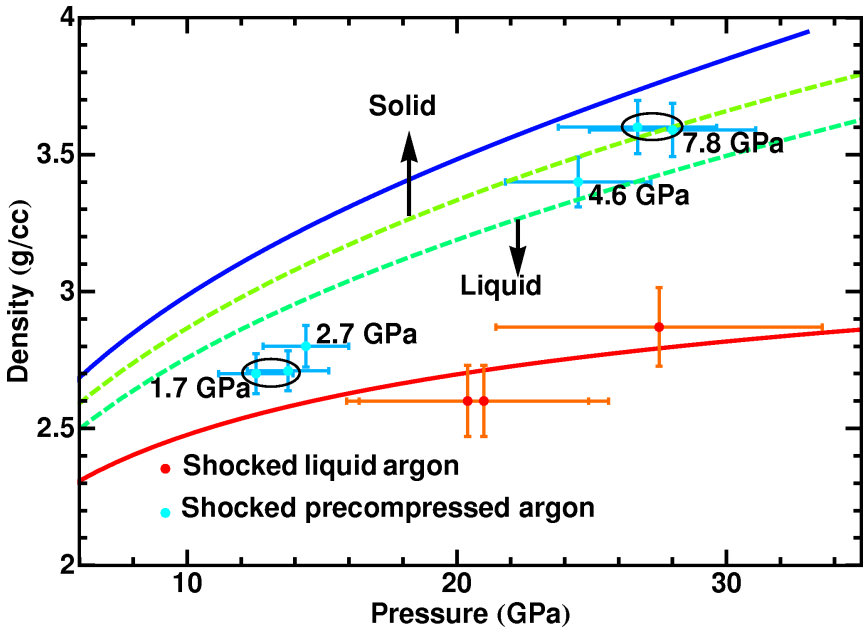

Fig. 5: The pressure and density of argon shocked from precompressed states (cyan points) and from the liquid state at 84 K (red points). The precompressed points are labeled by the initial applied pressure. The curves are the cryogenic (84 K) liquid argon Hugoniot in red, the calculated boundaries of the equilibrium liquid and solid states in green, and the room temperature isotherm in blue. Argon at equilibrium is liquid at densities below the dashed melt line.

demonstrating that an equilibrium shocked state can be established and characterized in argon within the duration of the experimental window.

We assume the initial density and refractive index of argon given by Grimsditch et al.[16], based on a measurement of the initial precompression via ruby fluorescence[34]. The aluminum ablation layer is fabricated by direct compression of aluminum between two diamonds.

Precompression changes the final shocked state via two qualitative effects. First, as the density and sound speed of the precompressed argon increases, the shock pressure transmitted from the aluminum ablator into the argon increases via improved shock impedance matching. Second, as the initial precompression increases, the degree of heating from a given shock compression decreases[15], increasing the shocked density. As precompression is increased, the Hugoniot approaches isentropic compression[6,15]. At constant pump fluence, we find a strong increase in shock pressure with precompression of argon, and an increase in density which approaches the room temperature isotherm for argon, shocked from a precompression of 7.8 GPa.

As the precompression is decreased, the final shocked state decreases in density faster than the melt line, approaching the cryogenic liquid argon Hugoniot. For solid argon shocked from a precompression of 1.7 GPa (argon at room temperature melts at 1.3 GPa), we observe a shocked density that is well below the density along

the melt line. Although this may indicate that shocked argon has melted, we note the possibility that a transient metastable state may also occur[7,17]. Further, inspection of the corresponding 1.7 GPa phase shift data in fig. 4 indicates that a characteristic sinusoidal oscillation (consistent with shock propagation) has begun within about 50 ps after the shock arrival at the Al/Ar interface, exhibiting a constant period consistent with steady propagation thereafter. Even if the shocked state of the 1.7 GPa data is metastable, on the time scale of this experiment the constant period of the data indicates that the shock wave has reached a steady state within 50 ps after arrival in the argon.

We note that the generated shock states can be varied over a region of phase space that is not easily accessible to single shock or static compression experiments. In combination with sample preheating and variation of the pump fluence, it should be possible to explore a much wider region of the material phase space off the standard room pressure Hugoniot.

In conclusion, we have observed shocked states off the room pressure Hugoniot by applying ultrafast shock wave techniques to argon that has been precompressed in a conventional diamond anvil cell. We have also developed a straightforward method for analyzing ultrafast shock wave data. Although our analysis is currently limited to non-metallic shock induced index of refraction changes of less than 0.9 (for an initial index of 1.4), with further development it should be possible to extend the analysis outside of this regime. Since this technique has ultrafast time resolution, it is possible to explore the early time dynamics of shock induced phase transitions and chemical reactions. By varying the initial pressure, we are able to significantly modulate the final shock temperature and pressure, greatly extending the thermodynamic phase space accessible to single shock experiments.

We acknowledge useful discussions with L. Fried, E. Glascoe, C. Grant, E. Reed, H. Lorenzana, C. Bolme, S. Mcgrane, and J. Forbes. This work was performed under the auspices of the U.S. Department of Energy by Lawrence Livermore National Laboratory under Contract DE-AC52-07NA27344 and funded in part by the DTRA Advanced Energetics program.

References

[1] Crowhurst, J. C., Brown, J. M., Goncharov, A. F., and Jacobsen, S. D., Elasticity of (Mg,Fe)O through the spin transition of iron in the lower mantle. *Science* **319**, 451 (2008).

[2] Zaug, J. M., Abramson, E. H., Brown, J. M., and Slutsky, L. J., Sound Velocities in Olivine at Earth Mantle Pressures. *Science* **260**, 1487 (1993).

[3] Nellis, W. J., Weir, S. T., and Mitchell, A. C., Metallization and electrical conductivity of hydrogen in Jupiter. *Science* **273**, 936 (1996).

[4] Nna-Mvondo, D., Khare, B., Ishihara, T., and McKay, C. P., Experimental impact shock chemistry on planetary icy satellites. *Icarus* **194**, 816 (2008).

[5] McGrane, S. D., Moore, D. S., and Funk, D. J., Shock induced reaction observed via ultrafast infrared absorption in poly(vinyl nitrate) films. *J. Phys. Chem. A* **108**, 9342 (2004).

[6] Nellis, W. J., Dynamic compression of materials: metallization of fluid hydrogen at high pressures. *Rep. Prog. Phys.* **69**, 1479 (2006).

[7] Kalantar, D. H. et al., Direct observation of the alpha-epsilon transition in shock-compressed iron via nanosecond x-ray diffraction. *Phys. Rev. Lett.* **95**, 075502 (2005).

[8] Dlott, D. D., Thinking big (and small) about energetic materials. *Mater. Sci. Technol.* **22**, 463 (2006).

[9] Bassett, W. A., Diamond anvil cell, 50th birthday. *High Pressure Research* **29**, CP5 (2009).

[10] Hemley, R. J., Effects of high pressure on molecules. *Annu. Rev. Phys. Chem.* **51**, 763 (2000).

[11] Grochala, W., Hoffmann, R., Feng, J., and Ashcroft, N. W., The chemical imagination at work in very tight places. *Anew. Chem., Int.* **46**, 3620 (2007).

[12] Smith, R. L. and Fang, Z., Techniques, applications and future prospects of diamond anvil cells for studying supercritical water systems. *J. Supercrit. Fluids* **47**, 431 (2009).

[13] Schettino, V. et al., Chemical Reactions at Very High Pressure. *Adv. Chem. Phys.* **131**, 105 (2005).

[14] Hoover, W. G., Structure of a Shock-Wave Front in a Liquid. *Phys. Rev. Lett.* **42**, 1531 (1979).

[15] Jeanloz, R. et al., Achieving high-density states through shock-wave loading of precompressed samples. *Proc. Natl. Acad. Sci. U. S. A.* **104**, 9172 (2007).

[16] Grimsditch, M., Loubeyre, P., and Polian, A., Brillouin-Scattering and 3-Body Forces in Argon at High-Pressures. *Phys. Rev. B* **33**, 7192 (1986).

[17] Ernstorfer, R. et al., The Formation of Warm Dense Matter: Experimental Evidence for Electronic Bond Hardening in Gold. *Science* **323**, 1033 (2009).

[18] Dlott, D. D., Ultrafast spectroscopy of shock waves in molecular materials. *Annu. Rev. Phys. Chem.* **50**, 251 (1999).

[19] Greenfield, M., McGrane, S. D., and Moore, D. S., Control of cis-Stilbene Photochemistry Using Shaped Ultraviolet Pulses. *J. Phys. Chem. A* **113**, 2333 (2009).

[20] Armstrong, M. R., Crowhurst, J. C., Reed, E. J., and Zaug, J. M., Ultrafast high strain rate acoustic wave measurements at high static pressure in a diamond anvil cell. *Appl. Phys. Lett.* **92**, 101930 (2008).

[21] Bolme, C. A., McGrane, S. D., Moore, D. S., and Funk, D. J., Single shot measurements of laser driven shock waves using ultrafast dynamic ellipsometry. *J. Appl. Phys.* **102**, 033513 (2007).

[22] Evans, R. et al., Time- and space-resolved optical probing of femtosecond-laser-driven shock waves in aluminum. *Phys. Rev. Lett.* **77**, 3359 (1996).

[23] Manheimer, W. M., Colombant, D. G., and Gardner, J. H., Steady-State Planar Ablative Flow. *Phys. Fluids* **25**, 1644 (1982).

[24] Barker, L. M. and Hollenbach, R. E., Shock-Wave Studies of Pmma, Fused Silica, and Sapphire. *J. Appl. Phys.* **41**, 4208 (1970).
[25] Kim, K. Y. et al., Single-shot, interferometric, high-resolution, terahertz field diagnostic. *Appl. Phys. Lett.* **88**, 041123 (2006).
[26] Geindre, J. P., Audebert, P., Rebibo, S., and Gauthier, J. C., Single-shot spectral interferometry with chirped pulses. *Opt. Lett.* **26**, 1612 (2001).
[27] Benuzzi-Mounaix, A. et al., Chirped pulse reflectivity and frequency domain interferometry in laser driven shock experiments. *Phys. Rev. E* **60**, R2488 (1999).
[28] Gahagan, K. T. et al., Measurement of shock wave rise times in metal thin films. *Phys. Rev. Lett.* **85**, 3205 (2000).
[29] Kim, K. Y., Alexeev, I., and Milchberg, H. M., Single-shot supercontinuum spectral interferometry. *Appl. Phys. Lett.* **81**, 4124 (2002).
[30] Vanthiel, M. and Alder, B. J., Shock Compression of Argon. *J. Chem. Phys.* **44**, 1056 (1966).
[31] Ross, M., High-Density Fluid-Perturbation Theory Based on an Inverse 12th-Power Hard-Sphere Reference System. *J. Chem. Phys.* **71**, 1567 (1979).
[32] Kang, H. S. and Ree, F. H., A Variational Theory of Classical Solids. *J. Chem. Phys.* **99**, 2985 (1993).
[33] Ross, M., Mao, H. K., Bell, P. M., and Xu, J. A., The Equation of State of Dense Argon - a Comparison of Shock and Static Studies. *J. Chem. Phys.* **85**, 1028 (1986).
[34] Zha, C. S., Mao, H. K., and Hemley, R. J., Elasticity of MgO and a primary pressure scale to 55 GPa. *Proc. Natl. Acad. Sci. U. S. A.* **97**, 13494 (2000).